Giant Nonhysteretic Responses of Two-Phase Nanostructured Alloys

Wei-Feng Rao,[1] Manfred Wuttig,[2] and Armen G. Khachaturyan[1,*]

[1]*Department of Materials Science and Engineering, Rutgers University, Piscataway, New Jersey, 08854, USA*
[2]*Department of Materials Science and Engineering, University of Maryland, College Park, Maryland, 20742, USA*

(Received 11 October 2010; revised manuscript received 2 December 2010; published 10 March 2011)

A new class of functional materials with giant nonhysteretic strain responses to applied fields is considered. They are decomposed two-phase systems consisting of single-domain nanoprecipitates of a low-symmetry phase. Their strain response is caused by the field-induced change of structural orientation of the domain states of these precipitates. The superresponse follows from the novel concept of structural anisotropy that is analogous to the magnetic anisotropy. Its vanishing produces a new glasslike structural state. The developed phase field theory and modeling allow us to formulate criteria for searching superresponsive two-phase nanostructured alloys.

DOI: 10.1103/PhysRevLett.106.105703 PACS numbers: 64.70.kd, 64.75.Op, 81.30.Kf, 81.40.Cd

Two-phase nanostructured alloys, consisting of coherent nanoprecipitates of the low-symmetry phase from the cubic matrix, are well known for their excellent mechanical properties due to the precipitation hardening. However, they have never been considered as promising functional materials. In this Letter, we introduce a new concept of structural anisotropy to consider the effects of field-induced crystal lattice rearrangement on their strain responses. It is demonstrated that these materials can have remarkable strain responses to applied fields. In particular, they can have a combination of giant low- or nonhysteretic field-induced strain responses, high blocking forces, and good mechanical properties. This suggests that some nanodispersive two-phase alloys may be functionalized to have supreme properties.

To describe the crystal lattice rearrangement mode, we introduce a strain tensor, ε^0_{ij}, called conditional eigenstrain. The conditional eigenstrain, ε^0_{ij}, is a relaxing six-component long-range order parameter fully defined by three principal strains (eigenvalues) and three corresponding principal directions (eigenvectors). For a low-symmetry phase, the n symmetry-related energy minimizing structural states are characterized by $\varepsilon^0_{ij} = \varepsilon^{00}_{ij}(p)$, $(p = 1, 2, \ldots, n)$, where $\varepsilon^{00}_{ij}(p)$ are the stress-free Eshelby eigenstrains [1,2]. A transition between two states of $\varepsilon^{00}_{ij}(p)$ can be accomplished by small atomic displacements, which, for example, results in the 90° rotation of principal directions of ε^0_{ij} for the tetragonal phase, and does not require a 90° rotation of the entire lattice of the domain [Figure 1(a)]. A newly introduced notion of structural anisotropy is described by an energy function of the orientation of principal directions of ε^0_{ij}, which can be derived from the specific free energy, $f(\varepsilon^0_{ij})$, by its partial minimization with respect to eigenvalues of ε^0_{ij}.

The structural anisotropy is analogous to the magnetic anisotropy in ferromagnets, wherein the energy is directionally dependent on a vector (magnetization) rather than a tensor [3]. Like magnetic anisotropy that crucially influences main characteristics of ferromagnets [3], the structural anisotropy distinguishes structurally hard and soft materials, affects similar characteristics of structural materials, such as the width, size and mobility of structural domains, and determines the hysteresis.

To quantify the structural anisotropy, we approximate $f(\varepsilon^0_{ij})$ by a Landau polynomial [4,5]:

$$f(\varepsilon^0_{ij}) = \tfrac{1}{2}C_{ijkl}\varepsilon^0_{ij}\varepsilon^0_{kl} + \tfrac{1}{3}D_{ijklsm}\varepsilon^0_{ij}\varepsilon^0_{kl}\varepsilon^0_{sm} + \ldots, \quad (1)$$

where $\varepsilon^0_{ij} = 0$ describes the stress-free cubic parent phase; C_{ijkl} and D_{ijklsm} are tensor coefficients with the symmetry of the parent cubic phase, summation over repeated indices is implied. C_{ijkl} are elastic constants. In general, these coefficients are functions of temperature and composition.

The general behavior of $f(\varepsilon^0_{ij})$ can be illustrated in its subspace of uniaxial strain defined by $f = f(\varepsilon^*, \boldsymbol{n})$, where $\boldsymbol{n}$ is a direction of uniaxial ε^0_{ij}, and ε^* is a typical value of the strain while ratios between principal values of ε^0_{ij} are fixed. Figures 1(b)–1(d) show the surfaces $f = f(\varepsilon^*, \boldsymbol{n})$

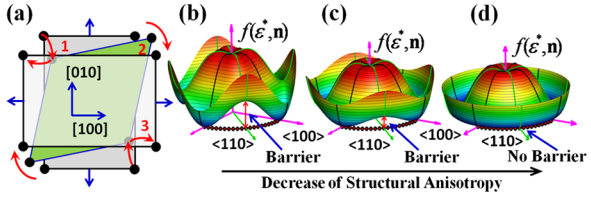

FIG. 1 (color online). (a) Schematic flipping of a tetragonal unit cell through small atomic displacements, and (b)–(d) the free energy dependence on the representative strain, ε^*, and direction $\mathbf{n}$ in the (001) plane. The transition, i.e., from 1 to 3, goes through intermediate states like 2 in (a), and a projection of the transition path is indicated by dots in (b)–(d). The red arrow in (b–d) shows the energy barrier along this path. A local minimum at the top of (b)–(d) (at $\varepsilon^* = 0$) describes the metastable parent phase.

for different structural anisotropies and $\boldsymbol{n}$ located in the (001) plane. Positions of global minima in Figs. 1(b) and 1(c) at $\boldsymbol{n} \parallel \langle 100 \rangle$ indicate that the stable phase is tetragonal. The value of the energy barriers between the minima determines the easiness of a rotational transition between them distinguishing structurally hard and soft materials. Application of the external fields can eliminate the barriers greatly reducing the hysteresis. Vanishing of the structural anisotropy, Fig. 1(d), eliminates the barriers and corresponds to a limit case of structural isotropy. This occurs when (1) becomes an expansion in invariants of ε^0_{ij}, which are $(\varepsilon^0_{ii})^2$, $\varepsilon^0_{ij}\varepsilon^0_{ij}$, $\varepsilon^0_{ij}\varepsilon^0_{jk}\varepsilon^0_{ki}$, $\varepsilon^0_{ij}\varepsilon^0_{ij}\varepsilon^0_{kk}$, and, etc., with scalar expansion coefficients. Since ε^0_{ij} in this case is "decoupled" from the crystallographic directions of the parent phase, an unusual structure consisting of structural nanodomains with all possible (spherically degenerated) orientations is resulted. This structure has infinite rotational flexibility, and can be perceived as structural glass that is analogous to the ferromagnetic glass.

The structural anisotropy discussed above is only an intrinsic part of the total anisotropy describing the free energy of the lattice rearrangement of ideal crystals. There is another source of structural anisotropy associated with the coherency strain required to restore the lattice compatibility. Its energy depends on the volume of the nanodomains, lattice orientation of precipitates, and their shapes and positions. Therefore, the extrinsic anisotropy is a structure-sensitive extrinsic property. In particular, it is described by the Khachaturyan-Shatalov theory [2,6]. The extrinsic anisotropy is analogous to the anisotropy produced by the magnetostatic energy described by the magnetic shape factor [7] that also depends on shapes and positions of magnetic particles [2,8]. In fact, this analogy is rooted in the mathematic similarity of both interactions [2,7,9].

In this Letter, we study the formation of mixture of the cubic and tetragonal phases obtained by decomposition during "annealing" of the supersaturated cubic solid solution, which was quenched into the two-phase region. We consider microstructures at very early stages of the growth and coarsening when dimensions of precipitates of the tetragonal phase are still within the nanoscale range. The strain response of the obtained systems to the applied stress is investigated (applied magnetic fields could be similarly considered). The nanosize of particles guarantees the single-domain state, and thus reduces a hysteresis by eliminating energy dissipation associated with domain wall movements. The evolution of composition, $c(\mathbf{r}, t)$, and conditional eigenstrain, $\varepsilon^0_{ij}(\mathbf{r}, t)$, are based on the phase field microelasticity kinetic equations [10]:

$$\frac{\partial \varepsilon^0_{ij}(\mathbf{r}, t)}{\partial t} = -L \frac{\delta F}{\delta \varepsilon^0_{ij}(\mathbf{r}, t)} + \xi_\varepsilon(\mathbf{r}, t), \tag{2a}$$

$$\frac{\partial c(\mathbf{r}, t)}{\partial t} = M\nabla^2 \frac{\delta F}{\delta c(\mathbf{r}, t)} + \xi_c(\mathbf{r}, t), \tag{2b}$$

where t is time, F is the total nonequilibrium free energy, $\delta F/\delta \varepsilon^0_{ij}$ and $\delta F/\delta c$ are the driving forces, L and M are the kinetic coefficients, and $\xi_\varepsilon(\mathbf{r}, t)$ and $\xi_c(\mathbf{r}, t)$ are Langevin noise terms. The total free energy functional is

$$\begin{aligned} F(\varepsilon^0_{ij}, c) = \int_V \Big(& f(\varepsilon^0_{ij}, c) + \frac{1}{2}\beta_\varepsilon \frac{\partial \varepsilon^0_{ij}}{\partial r_m}\frac{\partial \varepsilon^0_{ij}}{\partial r_m} + \frac{1}{2}\beta_c \frac{\partial c}{\partial r_m} \\ & \times \frac{\partial c}{\partial r_m}\Big) d^3 r + \frac{1}{2}\int (C_{ijkl} \\ & - n_m C_{ijmn}\Omega_{np}(\boldsymbol{n}) C_{klpq} n_q)\tilde{\varepsilon}^0_{ij}(\boldsymbol{k})\tilde{\varepsilon}^0_{kl}(\boldsymbol{k}) \\ & * \frac{d^3 k}{(2\pi)^3} - \int_V \sigma^{\mathrm{app}}_{ij}\varepsilon^0_{ij} d^3 r, \end{aligned} \tag{3}$$

where $f(\varepsilon^0_{ij}, c)$ is the anharmonic nonequilibrium energy density function, β_ε and β_c are the gradient coefficients. The second term is the coherency strain energy caused by the crystal lattice misfit associated with $\varepsilon^0_{ij}(\mathbf{r})$ [2,6], and the third term is the energy of interaction with the applied stress, σ^{app}_{ij}. $\tilde{\varepsilon}^0_{ij}(\mathbf{k})$ is the Fourier transform of $\varepsilon^0_{ij}(\mathbf{r})$, $\boldsymbol{n} = \boldsymbol{k}/k$ is the unit vector, and $\Omega_{mn}(\mathbf{n}) = (C_{mijn} n_i n_j)^{-1}$. In our modeling we write $f(\varepsilon^0_{ij}, c)$ as

$$\begin{aligned} f(\varepsilon^0_{ij}, c) = {} & A_0(c - c_1)^2(c - c_2)^2(1 + A_1 c + A_2 c^2) \\ & + \frac{1}{2}C_{ijkl}\varepsilon^0_{ij}\varepsilon^0_{kl} + \frac{c(r) - c_\alpha}{c_\beta - c_\alpha}\Big[\frac{B_{30}}{3}\varepsilon^0_{ij}\varepsilon^0_{jk}\varepsilon^0_{ki} \\ & + \frac{B_{33}}{3}(\varepsilon^0_{mm})^3 + \frac{D_{40}}{4}(\varepsilon^0_{ij}\varepsilon^0_{ij})^2 + \frac{D_{44}}{4}(\varepsilon^0_{mm})^4\Big], \end{aligned} \tag{4}$$

where the structural anisotropy enters only the quadratic terms in ε^0_{ij}, characterized by $\mu = C_{11} - C_{12} - 2C_{44}$, and other coefficients are scalars.

Equation (2) is solved in the reduced forms (denoted by superscript asterisk *): stress and strain are measured in units of ε_3, ($\varepsilon^{0*}_{ij} = \varepsilon_{ij}/\varepsilon_3$, $\sigma^{0*}_{ij} = \sigma_{ij}/C_{44}\varepsilon_3$, $\varepsilon_3 = (c_t - a_c)/a_c$ and $\varepsilon_1 = (a_t - a_c)/a_c$ where c_t, a_t, and a_c are lattice parameters of the teteragonal and cubic phases, respectively); the energy in unit of the typical strain energy, $\Delta f = C_{44}\varepsilon_3^2$; all lengths in units of the physical length, l ($r^* = r/l$); the time t in units of the typical diffusion time, τ ($t^* = t/\tau$).

We use $A_0{}^* = 7500$, $A_1{}^* = -4.5787$, $A_2{}^* = 5.5319$, $c_1 = 0.25$, $c_2 = 0.5$, $c_\alpha = 0.235$, $c_\beta = 0.52$, $\beta^*_c = 60$, $\beta^*_\varepsilon = 3.0$, $L^* = 50.0$, and $M^* = 1.0$ (for decomposition only), which estimates $l \sim 1$ nm and the size of particles $\sim$10 nm. Other reduced values are listed in the upper part of Fig. 2, which provide about the same minimum energy density at $\varepsilon^{0*}_{33} \sim 1.00$ and $\varepsilon^{0*}_{11} = \varepsilon^{0*}_{22} \sim -0.300$ for different $\mu^* = \mu/C_{44}$. The behavior of the chosen Landau free energy is shown in the lower part of Fig. 2. The results presented below are obtained by the use of the periodical boundary conditions.

μ/C_{44}	C_{11}/C_{44}	C_{12}/C_{44}	$B_{30}/\Delta f$	$B_{33}/\Delta f$	$D_{40}/\Delta f$	$D_{44}/\Delta f$
0.00	2.50	0.50	-26.8737	-3.7744	14.2461	132.346
-0.05	2.48	0.53	-26.7067	-3.7668	14.1888	131.389
-0.10	2.47	0.57	-26.6261	-3.7661	14.1832	130.769
-0.20	2.44	0.64	-26.3178	-3.7517	14.1832	129.489
-0.50	2.36	0.86	-25.3352	-3.7070	13.7416	123.674

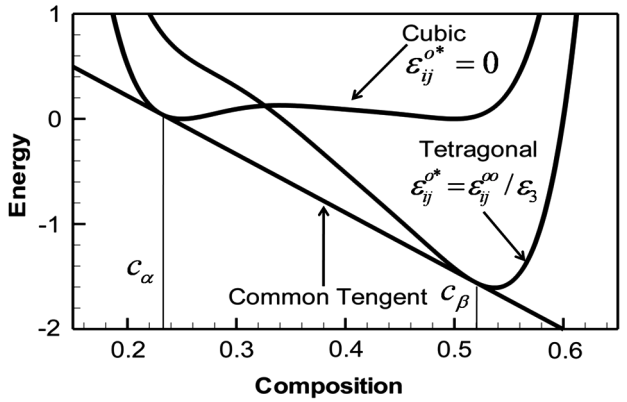

FIG. 2 (color online). Reduced parameters for different structural anisotropies (upper). Compositional dependence of the free energies of the cubic and tetragonal phases (lower).

Figure 3(a) shows a typical 3D microstructure formed by decomposition under constant uniaxial stress, where $\mu^* = -0.05$. Figure 3(b) shows the strain responses generated by the rotation of tetragonality axis under periodical uniaxial stresses. In addition to the conventional Hookean strain ($\varepsilon_{kl} = C^{-1}_{ijkl}\sigma_{ij}$), this rotational strain is calculated by the rotation of ε^0_{ij}, as $\Delta\bar{\varepsilon}_{ij} = \frac{1}{V}\int \Delta\varepsilon^0_{ij}(r)d^3r$ in the homogeneous modulus approximation [1,2]. Figure 3(b) thus shows that macroscopic strain responses are significantly magnified by the rotational flexibility of nanoparticles, which is recoverable and can be nonhysteretic. In fact, since $\Delta\bar{\varepsilon}_{ij} \sim \Delta\varepsilon^{00}_{ij}\omega$, $\Delta\varepsilon^{00}_{ij} \sim \varepsilon^{00}_{ij}$ and ε^{00}_{ij} can be up to $\sim$10%, $\Delta\bar{\varepsilon}_{ij}$ can thus be regarded a giant strain, where ω is the volume fraction of the rotated low-symmetry phase [2,11].

Further 2D modeling of the nanostructure formation without applying stress during decomposition shows that decreasing structural anisotropy increases the stress-induced deviation of the principal directions of ε^0_{ij} from the $\langle 10\rangle$ directions. In the limit isotropic case, $\mu^* = 0$, the structure is glasslike: its nanoprecipitates have random orientation of the principal directions of ε^0_{ij} (Fig. 4). The modeling also shows that if $\mu^* \geq -0.2$ and the stress is applied along the $\langle 10\rangle$ directions, the rotational strain becomes nonrecoverable. However, as in Fig. 5, the strain responses to stress applied along the $\langle 11\rangle$ directions are practically nonhysteretic for all simulated cases: the higher the structural anisotropy, the bigger the blocking force and the narrower the hysteresis loop.

Prototyping strain responses caused by rotational flexibility of the low-symmetry phase becomes possible only

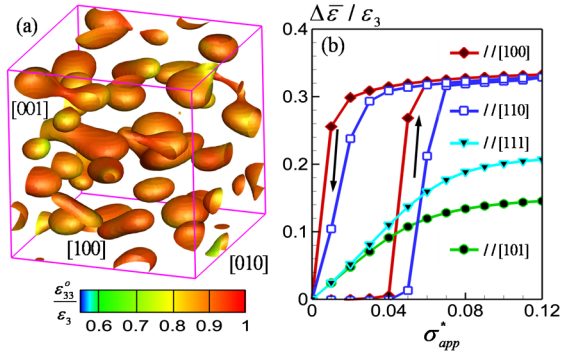

FIG. 3 (color online). (a) Microstructure obtained by decomposition under constant stress, and (b) strain responses induced by the rotation of ε^0_{ij} to periodically applied stress along different directions. The simulation size is $80 \times 80 \times 80$, $\bar{c} = 0.29$, $\mu^* = -0.05$ and $t^* \sim 8.8$. The constant stress applied during decomposition, $\sigma^*_{\text{app}} = 0.03$, is applied along [001].

after we introduce the relaxing conditional eigenstrain, ε^0_{ij}. This is an additional degree of freedom to the conventional Eshelby theory of coherent inclusions with fixed eigenstrain [1,2]. In fact, the Eshelby theory corresponds to a limiting case of infinitely ''hard'' materials.

While Eq. (1) defines the intrinsic structural anisotropy, the extrinsic structural anisotropy is provided by the coherency elastic strain, which stabilizes the initial configuration, modifies energy barriers for rotating ε^0_{ij}, and changes the blocking force. To minimize the hysteresis, we have to consider both intrinsic and extrinsic contributions to the energy barriers that are responsible for the hysteresis and recoverability.

A generic way to this goal is to apply stress along the $\langle 111\rangle$ direction (or $\langle 11\rangle$ direction in 2D). In this case, instead of flipping between $\langle 100\rangle$ domains, the stress rotates ε^0_{ij} of all particles toward the common $\langle 111\rangle$ direction, without overcoming any intrinsic energy barrier. Our computer modeling shows that the surmounted extrinsic energy barriers are also minimized in this case, which leads to practically monotonically increasing the total energy

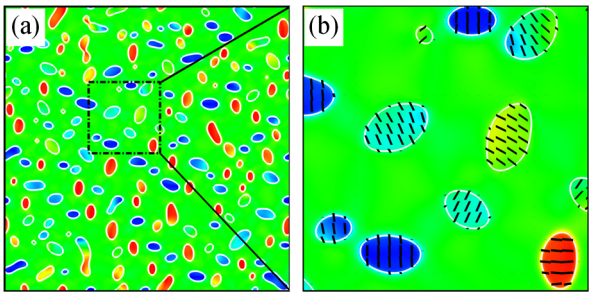

FIG. 4 (color online). (a) 2D microstructure of structurally isotropic system ($\mu = 0$) and (b) an inset of (a). Nanoparticles are bordered by white lines. In (b) the principal directions of ε^0_{ij} corresponding to its maximum principal value is shown by streaks. Simulation size is 512×512, $\bar{c} = 0.29$, $t^* \sim 24$, and no stress is applied during decomposition.

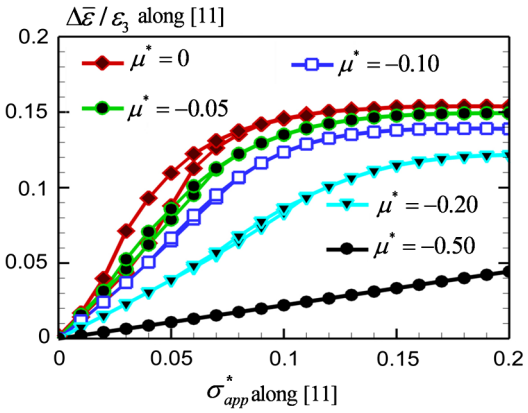

FIG. 5 (color online). Strain responses induced by the rotation of ε^0_{ij} to periodical stress applied along the [11] direction. The microstructures are obtained by 2D modeling of decomposition without applying stress. 2D simulation size is512×512, $\bar{c} = 0.29$ and $t^* \sim 24$.

upon deviation of ε^0_{ij}. Removing the stress thus relaxes ε^0_{ij} to its initial configuration, manifested as recoverable and nonhysteretic or weakly-hysteretic strain responses. In fact, similar arguments are even applicable to any tetragonal single crystal and single phase system, including single phase martensitic systems with multidomain structure.

For some microstructure engineered cases, there are alternative ways to minimize hysteresis. The [001] oriented domains are predominantly formed by decomposition under the [001] oriented stress [Fig. 3(a)]. Hence, there is no flipping of tetragonality under stress applied along [101] direction. Instead, it just rotates [001] domains toward [101]. This rotation is barrierless and thus has no hysteresis [Fig. 3(b)].

There are experimental findings consistent with our theory and modeling. About seven-fold strain softening—a strain increase at the same stress—is observed in the Fe-30%Pd alloy in a premartensitic two-phase state, which has been related to the formation of nanodispersions of tetragonal particles in the cubic matrix (tweed structure) [12]. The elastic softening associated with a displacive reorientation of randomly distributed nanodomain particles was reported in doped shape memory NiTi alloys [13,14]. We may also speculate that the nonhysteretic stress-induced rotation of tetragonality directions of the observed nanoprecipitates is the origin of the high elastic limit of the classical precipitation hardening Cu-Be alloy with the tweed structure [15]. A significant shape memory effect (SME) was recently discovered in this alloy [16]. It is also possible that the giant pseudoelastic deformation ($\sim 2.3\%$), and high strength observed in Gum Metals based on Ti-Nb alloys [17–19] are of the same nature.

In summary, specially chosen two-phase nanostructured alloys may have giant nonhysteretic strain responses to applied stress, excellent mechanical properties due to the precipitation hardening, and important martensitic features (SME and superelasticity). Such materials can also have giant magnetostriction if they are magnetic and the reorientation of single-domain states of nanoprecipitates is induced by magnetic field. The proposed theory and modeling provide a guideline for developing a new class of functional materials with giant nonhysteretic strain response, large blocking force, and good mechanical properties.

A. G. K. and W. F. R. gratefully acknowledge the support of DOE DE-FG02-06ER4629. M. W. was supported by NSF DMR-0705368 and MURI 28D1083899. The simulations were performed on LoneStar at TACC.

*Corresponding author.
khach@jove.rutgers.edu

[1] J. D. Eshelby, Solid State Phys. **3**, 79 (1956).
[2] A. G. Khachaturyan, *Theory of Structural Transformations in Solids* (Wiley & Sons, New York, 1983).
[3] G. Engdahl, *Handbook of Giant Magnetostrictive Materials* (Academic Press, San Diego, 2000).
[4] E. K. H. Salje, *Phase Transformations in Ferroelastic and Co-elastic Crystals* (Cambridge University Press, Cambridge, England, 1993).
[5] A. E. Jacobs, Phys. Rev. B **52**, 6327 (1995); A. E. Jacobs, S. H. Curnoe, and R. C. Desai, Phys. Rev. B **68**, 224104 (2003).
[6] A. G. Khachaturyan and G. A. Shatalov, Sov. Phys. Solid State **11**, 118 (1969).
[7] J. A. Osborn, Phys. Rev. **67**, 351 (1945).
[8] Y. M. Jin, Acta Mater. **57**, 2488 (2009).
[9] J. Slutsker and A. L. Roytburd, Phase Transit. **79**, 1083 (2006).
[10] Y. Z. Wang, H. Y. Wang, L. Q. Chen, and A. G. Khachaturyan, J. Am. Ceram. Soc. **76**, 3029 (1993); **78**, 657 (1995); Y. Z. Wang and A. G. Khachaturyan, Acta Mater. **45**, 759 (1997); Y. Ni and A. G. Khachaturyan, Nature Mater. **8**, 410 (2009).
[11] A. G. Khachaturyan and D. Viehland, Metall. Mater. Trans., A **38**, 2317 (2007).
[12] S. Muto, R. Oshima, and F. E. Fujita, Acta Metall. Mater. **38**, 685 (1990); H. D. Chopra and M. Wuttig, J. Phys. IV **05**, C8-157 (1995).
[13] Y. Murakami, H. Shibuya, and D. Shindo, J. Microsc. **203**, 22 (2001); Y. Murakami and D. Shindo, Philos. Mag. Lett. **81**, 631 (2001); D. Shindo, Y. Murakami, and T. Ohba, MRS Bull. **27**, 121 (2002).
[14] S. Sarkar, X. Ren, and K. Otsuka, Phys. Rev. Lett. **95**, 205702 (2005); Y. Wang, X. Ren, and K. Otsuka, Phys. Rev. Lett. **97**, 225703 (2006).
[15] L. E. Tanner, Philos. Mag. **14**, 111 (1966).
[16] H. Era, K. Kishitake, and K. Naito, Metall. Mater. Trans., A **31**, 2765 (2000).
[17] T. Saito *et al.*, Science **300**, 464 (2003).
[18] S. Kuramoto *et al.*, Metall. Mater. Trans., A **37**, 657 (2006).
[19] J. W. Morris *et al.*, Acta Mater. **58**, 3271 (2010).